

Article

High-Density Hydrogen Storage in a 2D-Matrix from Graphene Nanoblister: A Prospective Nanomaterial for Environmentally Friendly Technologies

Michael M. Slepchenkov, Pavel V. Barkov and Olga E. Glukhova * 

Department of Physics, Saratov State University, Astrakhanskaya Street 83, 410012 Saratov, Russia; slepchenkovmm@yandex.ru (M.M.S.); barkovssu@mail.ru (P.V.B.)

* Correspondence: glukhovaoe@info.sgu.ru; Tel.: +7-8452-514-562

Received: 31 January 2018; Accepted: 2 April 2018; Published: 6 April 2018



Abstract: In this paper, the atomic structure and mechanical stability of a new structural graphene modification—a 2D matrix of nanoscale cells in the form of a few-layer graphene substrate and nanoblister of a graphene monolayer—were studied for the first time. It is shown that such matrices are mechanically stable and are promising for environmentally friendly technologies. The calculated local atomic stress fields demonstrate that the atomic framework is not destroyed, even in the presence of defects in the atomic network of graphene nanoblister (Stone-Wales defect, double vacancies defect, ad-dimer defect, and their combination). However, it was established that the presence of one or more SW defects leads to the appearance of critical stresses. These critical stresses can induce local bond breaking in the atomic network with an increase in temperature or external pressure. It was found that graphene nanoblister can store molecular hydrogen with a maximum density of 6.6 wt % for 1158 m²/g at 77 K under normal pressure.

Keywords: graphene nanoblister; 2D matrix; mechanical stability; local stress field; defects; hydrogen storage

1. Introduction

Nanosystems/materials are currently being utilized to solve many significant scientific and technological problems worldwide. One of the challenges that can be approached with nanosystems is high-density hydrogen storage for use in environmentally friendly energy production. It is predicted that the potential areas of application for high density hydrogen storage systems could include the creation of ecological cars with next-generation fuel cells, as well as applications in the hydrogen power industry. Among the various low-dimensional carbon materials considered as promising hydrogen storage systems, preference is given to 2D structures, including graphene and its derivatives because of their high strength and adhesiveness. In the last few years, the direction devoted to experimental and theoretical studies of graphene nanoblister has been developing intensively. Blister structures are graphene layers with one or more pronounced islands of round shape formed in the atomic graphene grid. Structures of this type are formed on the surface of highly oriented pyrolytic graphite or epitaxial graphene when they are treated with atomic gaseous hydrogen [1–3].

The appearance of nanoblister as a new allotropic form of graphene was initially aimed at increasing its adhesive properties. The first mention of graphene nanoblister was associated with experimental studies of the adhesive properties of graphene membranes [4]. It is known that the blister test technique is widely used to evaluate the mechanical properties of thin films, as well as the adhesion energy between films and substrates [5]. The blister test method was first used to study the adhesive properties of membranes of atomic thickness in a work by Koenig et al. [6]. As an independent carbon

nanomaterial, graphene nanoblister were first considered in a work by Yuk et al., where the authors developed a new type of liquid cell for in situ transmission electron microscopy based on entrapment of a liquid film between layers of graphene [7]. New nanodevices based on graphene nanoblister are being actively developed. For example, a new type of ultrathin thermal engine based on graphene nanoblister has been proposed [8]. Weakly chemisorbed ClF_3 molecules are used as a high-power driver in the engine design. The proposed engine makes it possible to obtain a gasification pressure in the order of 22.9 GPa per operation cycle, demonstrates high reliability, and is not destroyed even after 10,000 operating cycles. It is predicted that graphene nanoblister will find wide applications in the creation of various nanomechanical devices, in particular, mechanical resonators [9]. In order to expand the spectrum of practical application of graphene nanoblister, it is necessary to evaluate the energy stability of blister structures and the influence of nanoblister topology. In this paper, we propose a new method for estimating the energy stability of graphene nanoblister based on the analysis of local stress distribution in the blister atomic network according to the original calculation algorithm, described in our previous work [10].

The purpose of this work is to identify the conditions for mechanical stability of the atomic network of graphene nanoblister with dimensions of several nanometers and a high packing density. The influence of structural defects on the mechanical stability of the graphene nanoblister and the maximum possible concentration of hydrogen stored by the nanoblister at normal pressure and low temperatures are also investigated.

2. Methods

In order to study a graphene nanoblister with a high packing density, we built an atomistic super-cell, which represents a few-layer graphene (as a substrate, the number of layers is 15) with a blister of a graphene monolayer. Graphene nanoblister is a convex monolayer. Figure 1a shows a super-cell where the silver layer represents the upper layer of a few-layer graphene substrate, and the green layer represents the blister of a graphene monolayer. The super-cell is translated in two directions X and Y, the cell sizes are 5.5×6.6 nm, respectively. The height of the convexity of graphene nanoblister is 0.9 nm. The tip of graphene nanoblister is presented in Figure 1b. The smallest distance of 3.2–3.4 Å between the nanoblister and the substrate is observed in the peripheral part of the super-cell (far from the convexity of graphene nanoblister).

The atomic structure of the super-cell was built in two stages. In the first stage, the AIREBO empirical potential [11] and the molecular dynamics method at a temperature of 70–90 K and normal pressure were applied. AIREBO potential allows us to adequately describe of a system of carbon and hydrogen atoms. The Nose-Hoover thermostat was used to regulate temperature in the considered system [12]. Integration of the motions equations was performed by the Verlet algorithm, which is traditionally used for these purposes in molecular dynamics [13]. All calculations were performed using the open-source KVAZAR [14]. In the second stage, the atomic structure of the super-cell was refined by the DFTB method using the DFTB+ software [15]. At present, the DFTB method is widely used to investigate the structural features of carbon nanostructures, including defect formation energy in graphene atomic grids [16]. It has been shown previously that the DFTB approach is able to successfully reproduce, with high quantitative accuracy, both structural and energetic data from full-density functional calculations at a fraction of the computational cost [17]. During model building, we used the results of the natural experiment on graphene nanoblister synthesis [18]. Figure 1c shows a 2D matrix obtained by translating the super-cell in two directions (X and Y). The density of the graphene nanoblister packing was 2.75×10^{12} atoms per 1 cm^2 .

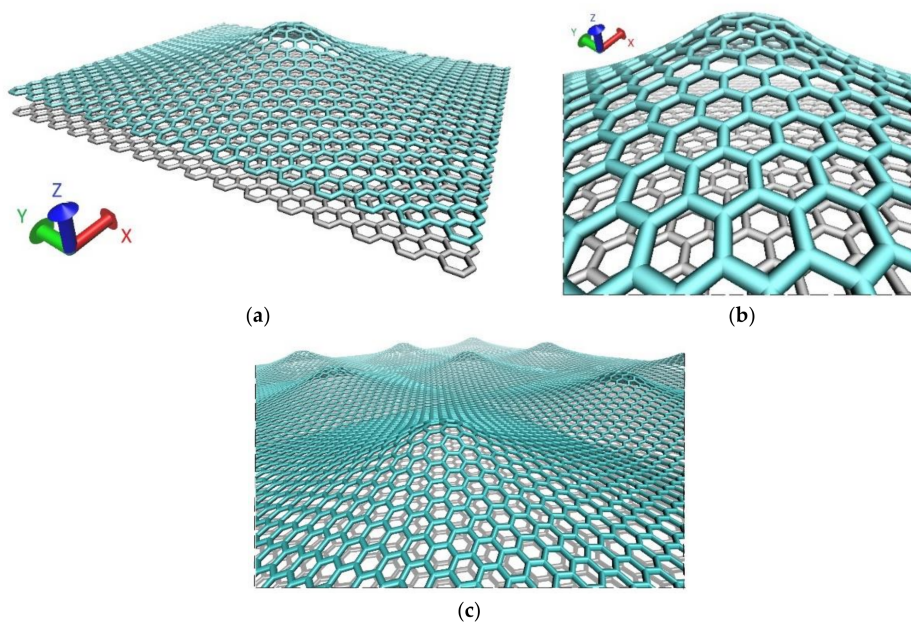


Figure 1. Atomic model of graphene nanoblister: (a) super-cell; (b) the tip of the nanoblister; (c) the overview of the nanoblister surface (the substrate is noted by silver color, the monolayer with graphene nanoblister is noted by blue color).

3. Results and Discussion

3.1. Mechanical Stability of the Atomic Network of Graphene Nanoblister with Defects

Since the synthesis of graphene modifications always produces defects in the atomic network, they can cause the appearance of nanocracks in the form of breaking C-C bonds. We considered Stone-Wells (SW) defects, double vacancy (2V) defects, Ad-dimer (AD) defects and multiple combinations of these defects in the nanoblister structure. To do this, appropriate defects were introduced into the atomic network, and then the atomic structure of graphene nanoblister was re-optimized by the DFTB method. As a result, the atomic network relaxes so that the graphene nanoblister energy is minimized again, corresponding to the ground state.

In some papers devoted to the structural features and properties of graphene nanoblister, researchers have focused on the mechanical properties of the surface and have used continuum mechanics approaches to investigate these properties [19]. Such estimates are not physically correct for graphene nanoblister, which are low-dimensional structures of atomic thickness and not objects of a continuous medium. At the same time, the methods and approaches of atomistic modeling have not previously been used to study graphene nanoblister. In these approaches, the energy of the structure is the main characteristic parameter that can be quantitatively estimated by means of a numerical experiment. We investigated the local atomic stress distribution using a previously developed method based on the energy approach [10]. The stress of the atomic network near the atom with number i σ_i was calculated by the formula:

$$\sigma_i = \left| w_i - w_i^0 \right|, \quad (1)$$

where w_i^0 is the volume energy density of the graphene nanoblister atom before the appearance of the defect; w_i is the volume energy density of the graphene nanoblister atom after the appearance of the defect. The volume energy density of the graphene nanoblister atom w_i was calculated by the formula within the AIREBO potential:

$$w_i = \left(\sum_{j \neq i} \left[E_{ij}^{REBO} + E_{ij}^{LJ} + \sum_{k \neq i, j, l \neq i, j, k} E_{kijl}^{tors} \right] \right) / V_i, \quad (2)$$

where E_{ij}^{REBO} is the interaction energy of covalently bonded atoms determined by the type of atoms and the distance between them; i and j are the numbers of interacting atoms; E_{kijl}^{tors} is the energy of the torsion interaction, which is a function of the linear dihedral angle built on the basis of atoms i,j,k,l with an edge at the bond $i-j$ (k,l —the atoms forming covalent bonds with atoms i,j); E_{ij}^{LJ} is the Van der Waals interaction energy between covalently non-bonded atoms; $V_i = 4/3\pi r_0^3$ is the volume occupied by atom i ; r_0 is the van der Waals radius of the carbon atom (1.7 Å). Numbers j,k enumerates all the atoms surrounding the given atom with the number i . Table 1 shows the calculated maximum values of local atomic stress σ_{max} for the graphene nanoblister with defects and the maximum values of bond length d_{max} . As can be seen from Table 1, the greatest stress in the atomic network of the graphene nanoblister occurs when at least one SW-defect appears. In these cases, the stress reaches 1.79–1.93 GPa, which corresponds to a critical value. Earlier, we showed that C-C bonds in graphene structures can be broken when stress reaches 1.8 GPa under the influence of external factors, such as an increase of temperature and pressure [10]. However, the other two defects—2V-defect and AD-defect—only increase the stress to 1.67–1.75 GPa, regardless of quantity and combination of defects. Therefore, these types of defects do not lead to destruction of the atomic network of graphene nanoblister, and graphene nanoblister with such defects can withstand increases in both pressure and temperature. The bond length distribution presented in Table 1 confirms that graphene nanoblister with defects is mechanically stable, since the maximum values of C-C bonds do not exceed 1.71 Å. As is known, the break of C-C bonds is observed at the bond length of 1.9 Å. Pictures of local atomic stresses for various defects are shown in Figure 2. Stress maps show how the stresses are distributed across the atoms of the graphene nanoblister network. The appearance of defects leads to an increase in stress not only at the top of the blister, but also in other local areas. An increase in stress near individual atoms also indicates that these atoms are more chemically active. Thus, the most curved local regions will more efficiently adsorb the atoms of hydrogen.

Table 1. Characteristics of investigated graphene nanoblister.

Type and Number of Defects	Maximum Values of Bond Length d_{max} , Å	Maximum Values of Local Atomic Stress σ_{max} , GPa
2V (1)	1.67 (2V)	1.75
2V (2)	1.67 (2V)	1.72
2V (3)	1.67 (2V)	1.67
AD (1)	1.67 (AD)	1.73
AD (2)	1.68 (AD)	1.72
AD (3)	1.67 (AD)	1.71
SW (1)	1.65 (SW)	1.82
SW (2)	1.69 (SW)	1.90
SW (3)	1.70 (SW)	1.91
AD (2) + 2V (1)	1.67 (AD) 1.67 (2V)	1.68
AD (2) + SW (1)	1.68 (AD) 1.70 (SW)	1.89
2V (2) + SW (1)	1.71 (2V) + 1.56 (SW)	1.93
2V (2) + AD (1)	1.67 (2V) + 1.64 (AD)	1.67
2V (1) + SW (1)	1.65(SW) + 1.67 (2V)	1.79
SW (1) + 2V (1) + AD (1)	1.65 (SW) + 1.70 (2V) + 1.68 (AD)	1.91
SW (1) + AD (1)	1.65 (SW) + 1.68 (AD)	1.86
2V (1) + AD (1)	1.67 (2V) + 1.65 (AD)	1.70
SW (2) + 2V (1)	1.64 (SW) + 1.70 (2V)	1.86
SW (2) + AD (1)	1.65 (SW) + 1.69 (AD)	1.79
2V (3)	1.67 (2V)	1.67

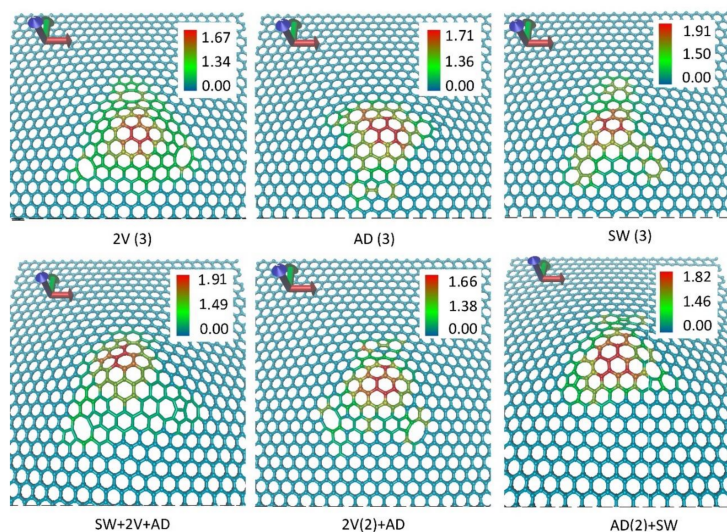


Figure 2. Maps of the local atomic stress of investigated graphene nanoblister for various defects. A calibration scale of stresses in GPa is indicated in the top right corner of each picture.

3.2. High-Density Hydrogen Storage in Graphene Nanoblister

Next, we investigated the process of filling graphene nanoblister with atomic hydrogen at normal pressure and 70–90 K. We used atomic hydrogen because earlier, in natural experiments, it was shown that in a layered graphite structure with inter-diagonal distance 2.5 Å, only atomic hydrogen with a Bohr radius of 0.5 Å is able to penetrate, while there is no possibility of penetration for molecular hydrogen with a diameter of 2.9 Å [20]. As in the case of the formation of the super-cell atomic framework, the molecular dynamics method on the base of AIREBO potential was applied in the first stage, and then the DFTB method was used to refine the super-cell configuration. The average temperature during the hydrogen accumulation in the blister was 77 K.

The concentration of hydrogen atoms increased in the blister as follows: (1) the cavity of graphene nanoblister (Figure 1a,b) was filled with a certain small amount of atomic hydrogen; (2) the super-cell was re-optimized; (3) the amount of hydrogen remaining in the graphene nanoblister, and its state and distribution in the nanoblister were determined. Furthermore, this three-stage procedure was repeated for a larger amount of atomic hydrogen. Figure 3a shows the example of filling graphene nanoblister with hydrogen for a concentration of 4.17 wt % (hydrogen is marked as blue). Two views of a 2D structure are presented in this figure: on the left—a perspective view; on the right—from above. At the initial stage, 1200 hydrogen atoms were chaotically located inside the cavity of the blister. After the process of molecular dynamic optimization, 768 atoms remained. The rest of the atoms were eliminated through the atomic network of graphene nanoblister. Analysis of the hydrogen atom distribution showed that hydrogen is concentrated mainly in the center of graphene nanoblister, while in the peripheral part (where the distance between the blister and the substrate is 3.2–3.4 Å), there is only 0.068 wt %. This is the hydrogen in atomic form when atoms formed chemical bonds with the substrate and the blister. The rest of the hydrogen—4.102 wt %—has passed into the molecular phase, as can be seen in Figure 3a.

The number of hydrogen atoms in graphene nanoblister was increased until the maximum density was reached. For current sizes of the super-cell and nanoblister height, the maximum hydrogen density was 6.86 wt % at a surface area of 0.8632 mg/m² (1158 m²/g). In this case, the amount of accumulated molecular hydrogen was 6.66 wt %. The atomic hydrogen was only 0.2 wt %. For comparison, the hydrogen adsorption vs surface area of bulk graphene-related materials with maximal value of ~5 wt % was achieved in [21] for a 0.4347 mg/m² (2300 m²/g) sample at the same temperature of 77 K. Figure 3b shows a view of graphene nanoblister with 6.86 wt % H (on the left—a perspective view; on the right—from above).

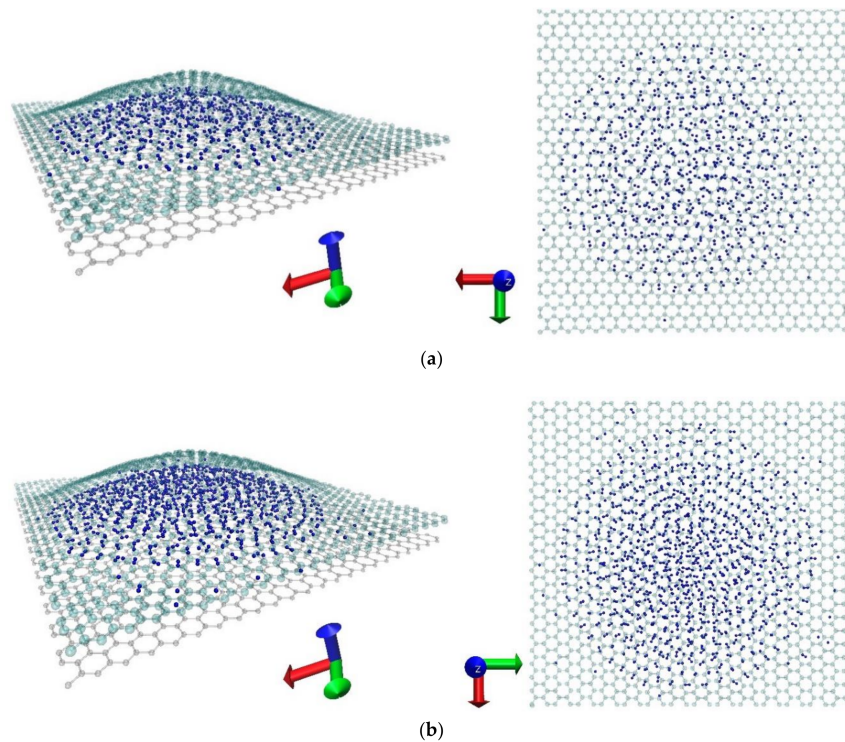


Figure 3. Hydrogen storage by graphene nanoblister: (a) a super-cell with 4.17 wt % of H-atoms; (b) a super-cell with 6.86 wt % of H-atoms (hydrogen atoms and molecules are noted by blue beads).

Numerical experiments performed with the filling of graphene nanoblister with defects showed that the defects do not affect the hydrogen filling process. We investigated the regularity in increasing the concentration of H atoms as a function of the surface density. Figure 4 shows the calculation results at a temperature of 77 K and an external pressure of 1 Bar. It was found that this regularity is non-linear; more precisely, it is exponential.

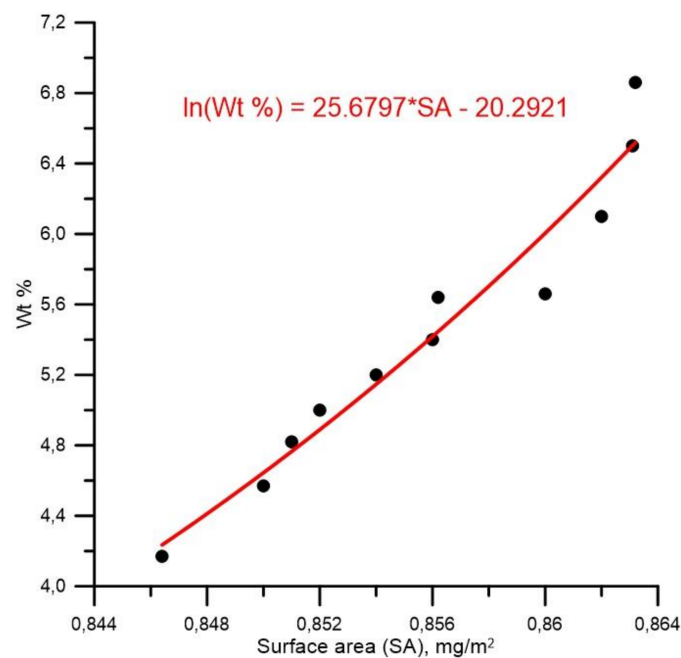


Figure 4. Hydrogen storage (wt %) versus surface area of graphene nanoblister sample at a temperature of 77 K and an external pressure of 1 Bar.

4. Conclusions

For the first time, we built an atomistic model of a 2D matrix structure of super-cells of graphene nanoblister and investigated the mechanical stability of this material. The density of nanoblister packing in the matrix was 2.75×10^{12} per 1 cm^2 . The super-cell was a few-layer graphene substrate with a nanoblister formed from a graphene monolayer. The size of the super-cell was $5.5 \times 6.6 \text{ nm}$, and the height of the nanoblister was 0.9 nm . The distance between the flat part of graphene nanoblister and the substrate was $3.2\text{--}3.4 \text{ \AA}$. Using the molecular dynamics method, AIREBO potential and the quantum-mechanical DFTB method, it was proved that the atomic network of graphene nanoblister retains its mechanical stability even in the presence of SW-defects, 2V-defects, AD-defects and their combinations. 2V and AD defects create the smallest perturbation in the local stress distribution in the atomic network of graphene nanoblister. These defects do not cause a critical stress in the atomic network regardless of quantity and combination of defects. They will not lead to the destruction of the framework with a slight (10–15%) increase in temperature and pressure.

The simulation of the process of filling graphene nanoblister with atomic hydrogen found the following: (1) the concentration (wt %) of H atoms in the nanoblister grows non-linearly (approximately exponentially) with increasing surface density; (2) the atomic network of the nanoblister does not collapse when its cavity is filled with hydrogen, even in the presence of defects; (3) the limiting density of stored molecular hydrogen is 6.6 wt % for $1158 \text{ m}^2/\text{g}$ ($0.8632 \text{ mg}/\text{m}^2$) for given nanoblister sizes ($5.5 \times 6.6 \text{ nm}$); (4) atomic hydrogen practically all becomes molecular in the process of filling the nanoblister.

From the results obtained in this study, it is concluded that such 2D matrices of graphene are extremely promising for storage of hydrogen and its transportation.

Acknowledgments: The work was supported by Russian Presidential scholarship 2016–2018 (project No. CII-3135.2016.1).

Author Contributions: Michael M. Slepchenkov and Olga E. Glukhova conceived and designed a method for calculating the local stress of atomic network of the blister; Pavel V. Barkov performed the numerical experiments; Michael M. Slepchenkov and Olga E. Glukhova analyzed the data; Michael M. Slepchenkov and Olga E. Glukhova wrote the paper.

Conflicts of Interest: The authors declare no conflict of interest.

References

1. Nechaev, Y.S.; Veziroglu, T.N. Thermodynamic aspects of the stability of the graphene/graphane/hydrogensystems, relevance to the hydrogen on-board storage problem. *Adv. Mater. Phys. Chem.* **2013**, *3*, 255–280. [[CrossRef](#)]
2. Watcharinyanon, S.; Virojanadara, C.; Osiecki, J.R.; Zakharov, A.A.; Yakimova, R.; Uhrberg, R.I.G.; Johansson, L.I. Hydrogen intercalation of graphene grown on 6H-SiC(0001). *Surf. Sci.* **2011**, *605*, 1662–1668. [[CrossRef](#)]
3. Lim, C.H.Y.X.; Sorkin, A.; Bao, Q.; Li, A.; Zhang, K.; Nesladek, M.; Loh, K.P. A hydrothermal anvil made of graphene nanobubbles on diamond. *Nat. Commun.* **2013**, *4*, 1556. [[PubMed](#)]
4. Huang, R. Graphene: Show of adhesive strength. *Nat. Nanotechnol.* **2011**, *6*, 537–538. [[CrossRef](#)] [[PubMed](#)]
5. Lee, C.; Wei, X.; Kysar, J.W.; Hone, J. Measurement of the elastic properties and intrinsic strength of monolayer graphene. *Science* **2008**, *321*, 385–388. [[CrossRef](#)] [[PubMed](#)]
6. Koenig, S.P.; Boddeti, N.G.; Dunn, M.L.; Bunch, J.S. Ultrastrong adhesion of graphene membranes. *Nat. Nanotechnol.* **2011**, *6*, 543–546. [[CrossRef](#)] [[PubMed](#)]
7. Yuk, J.M.; Park, J.; Ercius, P.; Kim, K.; Hellebusch, D.J.; Crommie, M.F.; Lee, J.Y.; Zettl, A.; Paul, A. Alivisatos High-Resolution EM of Colloidal Nanocrystal Growth Using Graphene Liquid Cells. *Science* **2012**, *336*, 61–64. [[CrossRef](#)] [[PubMed](#)]
8. Lee, J.H.; Tan, J.Y.; Toh, C.T.; Koenig, S.P.; Fedorov, V.E.; Castro Neto, A.H.; Özyilmaz, B. Nanometer Thick Elastic Graphene Engine. *Nano Lett.* **2014**, *14*, 2677–2680. [[CrossRef](#)] [[PubMed](#)]

9. Liao, P.; Xu, P. Effect of initial tension on mechanics of adhered graphene blisters. *Appl. Phys. A* **2015**, *120*, 1503–1509. [[CrossRef](#)]
10. Glukhova, O.; Slepchenkov, M. Influence of the curvature of deformed graphene nanoribbons on their electronic and adsorptive properties: Theoretical investigation based on the analysis of the local stress field for an atomic grid. *Nanoscale* **2012**, *4*, 3335–3344. [[CrossRef](#)] [[PubMed](#)]
11. O'Connor, T.C.; Andzelm, J.; Robbins, M.O. AIREBO-M: A reactive model for hydrocarbons at extreme pressures. *J. Chem. Phys.* **2015**, *142*, 024903. [[CrossRef](#)] [[PubMed](#)]
12. Evans, D.J.; Holian, B.L. The Nose–Hoover thermostat. *J. Chem. Phys.* **1985**, *83*, 4069. [[CrossRef](#)]
13. Grubmüller, H.; Heller, H.; Windemuth, A.; Schulten, K. Generalized Verlet Algorithm for Efficient Molecular Dynamics Simulations with Long-range Interactions. *Mol. Simul.* **1991**, *6*, 121–142. [[CrossRef](#)]
14. Glukhova Research Group. Available online: <http://nanokvazar.ru/en/kvazar> (accessed on 15 June 2017).
15. DFTB+. Available online: <https://www.dftbplus.org/> (accessed on 20 July 2017).
16. Skowron, S.T.; Lebedeva, I.V.; Popov, A.M.; Bichoutskaia, E. Energetics of atomic scale structure changes in graphene. *Chem. Soc. Rev.* **2015**, *44*, 3143–3176. [[CrossRef](#)] [[PubMed](#)]
17. Zobelli, A.; Ivanovskaya, V.; Wagner, P.; Suarez-Martinez, I.; Yaya, A.; Ewels, C.P. A comparative study of density functional and density functional tight binding calculations of defects in graphene. *Phys. Status Solidi B* **2012**, *249*, 276–282. [[CrossRef](#)]
18. Larciprete, R.; Colonna, S.; Ronci, F.; Flammini, R.; Lacovig, P.; Apostol, N.; Politano, A.; Feulner, P.; Menzel, D.; Lizzit, S. Self-Assembly of Graphene Nanoblisters Sealed to a Bare Metal Surface. *Nano Lett.* **2016**, *16*, 1808–1817. [[CrossRef](#)] [[PubMed](#)]
19. Wang, P.; Liechti, K.M.; Huang, R. Snap transitions of pressurized graphene blisters. *J. Appl. Mech.* **2016**, *83*, 071002. [[CrossRef](#)]
20. Waqar, Z. Hydrogen accumulation in graphite and etching of graphite on hydrogen desorption. *J. Mater. Sci.* **2007**, *42*, 1169–1176. [[CrossRef](#)]
21. Klechikov, A.G.; Mercier, G.; Merino, P.; Blanco, S.; Merino, C.; Talyzin, A.V. Hydrogen storage in bulk graphene-related materials. *Microporous Mesoporous Mater.* **2015**, *210*, 46–51. [[CrossRef](#)]



© 2018 by the authors. Licensee MDPI, Basel, Switzerland. This article is an open access article distributed under the terms and conditions of the Creative Commons Attribution (CC BY) license (<http://creativecommons.org/licenses/by/4.0/>).